



Mayfly Algorithm for Modelling a Horizontal Flexible Plate Structure

Aida Nur Syafiqah Shaari¹, Muhamad Sukri Hadi¹, Annisa Jamali^{2,*}, Intan Zaurah Mat Darus³

¹ School of Mechanical Engineering, College of Engineering, Universiti Teknologi MARA, 40450, Shah Alam, Selangor, Malaysia

² Faculty of Engineering, Universiti Malaysia Sarawak, 94300, Kota Samarahan, Sarawak, Malaysia

³ School of Mechanical Engineering, Universiti Teknologi Malaysia, 81310, Skudai, Johor, Malaysia

ARTICLE INFO

Article history:

Received 29 February 2024

Received in revised form 26 April 2024

Accepted 10 May 2024

Available online 30 May 2024

Keywords:

Modelling; Mayfly algorithm;
optimization; flexible structure; swarm
intelligence algorithm

ABSTRACT

Flexible plates are widely used in engineering and the industry, primarily due to the lightweight nature compared to rigid counterparts. These structures offer benefits such as cost savings, lower energy consumptions and improved operational safety. However, a notable drawback is that flexible structures are vulnerable to unwanted vibrations, which can cause structural damages. Hence, the development of specialized models are essential to effectively addressing this challenge. Researchers have devised various approaches to suppress unwanted vibrations, with contemporary studies often employing system identification techniques utilizing swarm intelligence algorithms to construct dynamic models of flexible structures. Therefore, this research employs the potent mayfly algorithm (MA), known for its effectiveness in optimization tasks. The developed models using MA were then compared with traditional approach known as recursive least square (RLS) through a comparative analysis. The outcome reveals that RLS exhibited the lowest mean square error (MSE) at 3.7392×10^{-6} , while MA had an MSE of 5.5185×10^{-6} . Yet, MA adeptly depicted the characteristics of the system, outperforming the RLS in these validation by indicating a 95% confidence level in the correlation test and exhibiting robust stability in the pole-zero diagram. Consequently, MA serves as a fitting algorithm to accurately depict the real behaviour of the flexible plate structure.

1. Introduction

In this modern technological era, the extensive utilization of flexible plate structures are evident across various engineering and industrial sectors including, aerospace, construction, maritime and energy [1-4]. These structures are favored for their exceptional structural and material properties. Notably, flexible structures are renowned for being lightweight, dependable, efficient, and capable of facilitating swift operations compared to rigid counterparts. Moreover, flexible structures come in diverse shapes and sizes. Presently, these structures play a pivotal role in manufacturing industries, offering advantages such as reduced labor requirements, cost-effectiveness, enhanced speed, ease of operation, and a decrease in workplace accidents [5]. However, despite their numerous merits,

* Corresponding author.

E-mail address: jannisa@unimas.my

<https://doi.org/10.37934/aram.118.1.167182>

flexible structures do have limitations, primarily related to their susceptibility to both internal and external disturbances, resulting in unwanted vibrations. This study aims to revolutionize the modelling of horizontal flexible plate (HFP) structures by introducing an intelligent approach, namely, the Mayfly Algorithm.

Unwanted or excessive vibrations pose a range of problems, such as machinery damage, diminished capability, bending, fatigue, and reduced overall performance. Hence, it is crucial to address and minimize these undesirable vibrations in flexible structures to maintain their optimal functionality. Therefore, to achieve this, the development of suitable models and effective control methods are essential, ensuring that flexible structures continue to play a significant role in various industries. Several approaches have been suggested by prior researchers and academic experts to address the concerns of undesired vibrations experienced by flexible plate structures [6]. Traditionally, passive vibration control (PVC) techniques have been employed to dampen excessive vibrations exerted towards such structures. Passive control can be applied in the form of mechanical solutions, such as incorporating vibration dampers or dynamic vibration absorbers into the system. However, passive control mechanisms are effective primarily in high-frequency range systems and tend to be less efficient in low-frequency ranges [7].

Furthermore, in engineering applications, greater emphasis is placed on utilizing lightweight systems. The inclusion of dampeners could lead to an increase in overall system weight, making it impractical. More recently, active vibration control (AVC) techniques have gained attention as a promising approach to reduce and manage vibrations, given their higher efficiency and reliability [8-9]. Hence, to address the limitations of passive vibration control (PVC) techniques, this research introduces an active vibration control (AVC) approach. However, before an effective controller can be developed for vibration suppression in a flexible plate system, it is crucial to create an accurate model of the structure. System identification (SI) techniques have emerged as the preferred method to determine the most suitable model structure.

SI involves constructing a mathematical model of the dynamic system based on collected vibration data [10]. The parameter estimation to construct mathematical model can be acquired from traditional and optimization approaches. Nonetheless, in situations where obtaining a model structure using traditional techniques proves challenging, intelligent methods become a desirable option [11-13]. Various forms of artificial intelligence, including glowworm swarm optimization (GSO), neural network systems, and mayfly algorithm (MA), have proven effective in parameter identification [8]. MA algorithm has been extensively studied for optimization and system identification across diverse applications, included but not confined to the automotive industry, engineering, function optimization, and task scheduling [14-16].

Mayflies belong to the Ephemeroptera order and are fragile insects renowned for their brief existence [17]. There are more than 3100 identified species of mayflies globally, and they spend nearly a year in anticipation of their brief emergence, with most having a lifespan of just one day. Their primary focus is on reproduction, often neglecting the need for food. Male mayflies form swarms for mating, which can vary in size from a few individuals to hundreds. These swarms form at an altitude of 1 to 4 meters above the ground and last for approximately 1.5 to 2 hours in the early morning. During this time, male mayflies engage in a distinctive up-and-down nuptial dance. After the dance, the males approach the females within the swarms, and the pairs descend into vegetation to mate before flying away separately.

This idea has been transformed into an optimization technique known as the MA. The algorithm is constructed by integrating elements from firefly algorithm (FA), particle swarm optimization (PSO) and genetic algorithms (GA) [18-20]. By incorporating the strengths of each of these approaches, the MA algorithm was devised. In this algorithm, it is assumed that every candidate is an adult ready for

breeding upon hatching. Candidates with the most superior values, irrespective of their lifespan, are the survivors in MA. Furthermore, the MA employs a diverse search strategy to achieve the optimal solution, involving artificial male and female mayflies. Additionally, the algorithm produces pairs of mayflies with an initial velocity of zero. This feature of diverse search procedures within MA facilitates the acquisition of the best possible solution according to the preset threshold [21].

Due to the increasing complexity of employing traditional methods to model flexible structures, there has been a notable shift towards the adoption of heuristic algorithm-based approaches in recent times. Hence, the primary objective of this study is to demonstrate the modelling of horizontal flexible plate (HFP) structure using an intelligence approach namely, MA. The novelty of this study lies in its departure from traditional modelling methods for flexible structures, which have become increasingly complex to implement. Instead, the research embraces a contemporary approach by employing heuristic algorithm-based techniques. Specifically, the study introduces the innovative use of the MA to model HFP structures. The experimental setup involved an aluminium rectangular plate with all clamped (CCCC) boundary conditions on all edges. Vibration was induced onto the plate by exciting it with a piezoelectric patch, and the purpose of this experiment was to gather input-output data from the system. Subsequently, this data will be employed in the development of a system model using system identification methods. Specifically, for the traditional approach, the model will be constructed using recursive least squares (RLS) for comparison purpose with intelligence approach namely, MA. Both models will undergo a comparison and validation process using evaluation metrics such as mean square error (MSE), pole-zero diagrams, and correlation tests within a 95% confidence interval.

2. Methodology

2.1 Experimental Setup

This study involves a comprehensive vibration data collection to evaluate the physical state of a horizontal flexible plate (HFP) system which entails employing transducers, namely sensors and actuators, signal conditioning equipment, and a computer operated with a DAQ system. In the development of the experimental rig for the HFP, actuators and sensors were affixed to the rig, enabling the collection of experimental vibration data. The experiment employed a square-shaped, flat, and thin aluminum plate measuring 0.7m on each side and 0.001m in thickness to represent the flexible system. In addition, the experimental plate rig was oriented horizontally to induce vertical vibrations onto the flexible plate. Complete specifications of the flexible plate utilized in this investigation are specified in Table 1 [6].

Furthermore, the experimental rig was configured with clamped edges on all sides. The generation of actuation force involved positioning a magnetic shaker precisely 1 cm parallel to the permanent magnet at the designated excitation point on the experimental setup. This magnetic shaker was meticulously controlled via a function generator, employing a power amplifier to create a sinusoidal force, thereby stimulating the system. Two piezo-beam type accelerometers were strategically positioned at separate locations across the experimental rig, functioning to capture the acceleration signal from the system. These accelerometers were carefully positioned at specific locations denoted as observation and detection points, as depicted in Figure 1 (a). These accelerometers were directly linked to the data acquisition system (PCI 6259) located within the computer, connected to an SCC-68 via a shielded cable through the PCI-bus. A fully assembled experimental configuration utilized in this research is depicted in Figure 1 (b) [6].

Table 1
 The properties of experimental plate [6]

No	Parameters	Numerical value
1.	Length, a	0.7 m
2.	Width, b	0.7 m
3.	Thickness, t	0.001 m
4.	Young's modulus, E	71.1 Gpa
5.	Poison ratio, ν	0.3
6.	Density, ρ	$2.71 \times 10^3 \text{ kg/m}^3$

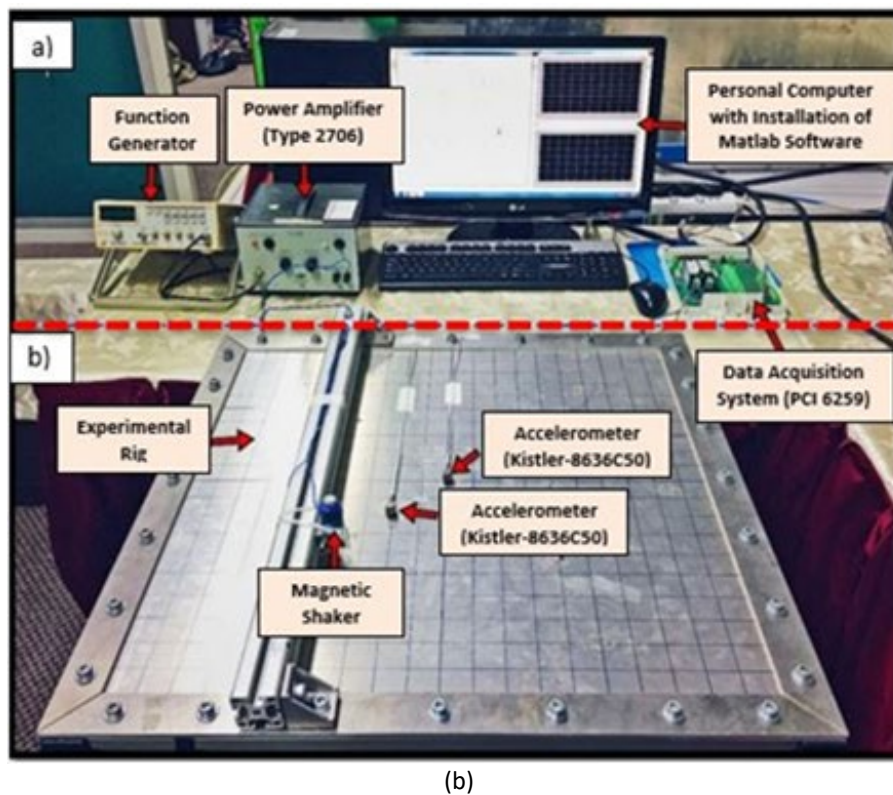
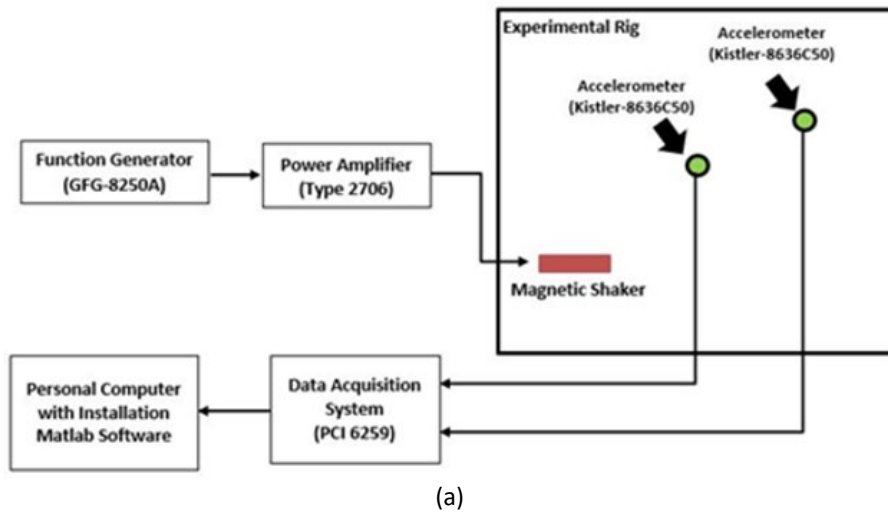


Fig. 1. System integration for vibration data collection of HFP structure in (a) experimental layout and (b) actual experimental setup [6]

2.2 System Identification

In this study, a swarm intelligence algorithm and traditional approaches were utilized to model the dynamic behavior of a HFP system with all clamped edges as boundary conditions. The parametric modelling was carried out employing the RLS and MA, utilizing a linear auto-regressive with exogenous input (ARX) model structure. These models were formulated based on actual experimental vibration data acquired from the experimental setup [6].

2.2.1 Mayfly algorithm

The MA is a relatively recent population-based method introduced in 2020 by Zervoudakis and Tsafarakis [22]. As mentioned earlier, MA draws inspiration from PSO and combines the strengths of PSO, firefly algorithm (FA), and genetic algorithm (GA). The algorithm operates in the following manner: Initially, two groups of mayflies are generated randomly, representing the male and female populations, respectively. Each mayfly is placed randomly within the problem space, serving as a candidate solution represented by a d -dimensional vector denoted as $P = (P_1, \dots, P_d)$. The alteration of mayflies is determined by velocity, $V = [V_1, V_2, \dots, V_d]^T$. The direction of movement is influenced by a combination the mayflies individual experiences and their interactions within the group. Primarily, these mayfly candidates adjust their positions toward two key points: their own best positions (p_{best}) and the best position identified within the group (g_{best}). The performance of these mayflies is then assessed based on a predefined fitness function, $f(x)$. In this study, the fitness function is defined by the minimum mean squared error (MSE) value as shown in Eq. (1) [6].

$$\min MSE = \frac{\sum_i^n (y(n) - \hat{y}(n))^2}{2} \quad (1)$$

In the context of the MSE equation, n refers to the number of data points in the dataset being analysed. Meanwhile, \hat{y} represents the predicted values, and y signifies the actual vibration data acquired from the experiment. These elements are utilized in the computation of the MSE. In MA, the algorithm operates through three main steps, which are;

i) Movement of male mayflies

Let P_i^t represent the original location of the i -th mayfly in specific search dimension at time step, t , with its location altered by the addition of the velocity, V_i^{t+1} and the current location. This relationship is represented by Eq. (2) [22].

$$P_{i,male}^{t+1} = P_i^t + V_i^{t+1} \quad (2)$$

where $x_{i,male}^0 \sim U(P_{min,male} - P_{max,female})$. Since male mayflies stay a few meters above water surface while performing their nuptial dance, it is believed that they unable to travel at high speeds and instead move at a constant pace. Consequently, the velocity of a male mayfly i can be described by Eq. (3) [22].

$$V_{ij}^{t+1} = V_{ij}^t + a_1 e^{-\beta r_p^2} (p_{best_{ij}} - P_{ij}^t) + a_2 e^{-\beta r_g^2} (g_{best_j} - P_{ij}^t) \quad (3)$$

where V_{ij}^t denotes the velocity of a male mayfly in dimension j (where $j = 1, 2, \dots, n$) at time step t . Next, P_{ij}^t represents the position of the i -th male mayfly in dimension j at the current time. The parameters a_1 and a_2 are constants used to scale the contributions of the local and global searches, respectively. Here, β indicates a fixed coefficient of visibility that is used to bound the visibility of the mayfly from other mayflies, while r_p is the representation of Cartesian distance between female and male mayflies. Additionally, $pbest_{ij}$ represents the personal best position of the mayfly. The calculation of the personal best position $pbest_{ij}$ at the subsequent time step, $t+1$, is given by Eq. (4) [22].

$$pbest_i = \begin{cases} P_{i,male}^{t+1}, & \text{if } f(P_{i,male}^{t+1}) > f(pbest_i) \\ \text{is kept the same,} & \text{otherwise} \end{cases} \quad (4)$$

where the cost function, denoted as $f: \mathbb{R}^n \rightarrow \mathbb{R}$, assesses the quality of the solution. The expression for the global best position $gbest$ at time step t is provided in Eq. (5) [22].

$$gbest \in \{pbest_1, pbest_2, \dots, pbest_N | f(cbest)\} = \min \{f(pbest_1), f(pbest_2), \dots, f(pbest_N)\} \quad (5)$$

where N represents the total count of male mayflies. Next, the distances between male mayfly position and current local best position can be computed using Eq. (6) [22].

$$\|P_{i,male} - P_{i,male}\| = \sqrt{\sum_{j=1}^n (P_{ij,male} - P_{ij,male})^2} \quad (6)$$

In this context, $P_{ij,male}$ represents the j -th element of mayfly i , and $P_{i,male}$ corresponds to either $pbest_i$ or $gbest$. Specifically, each mayfly adjusts its trajectory towards its personal best ($pbest$) obtained thus far, as well as the global best position achieved by the entire swarm ($gbest$). Adding a stochastic element to the algorithm, the best mayflies perform a nuptial dance at a given time. This dance is mathematically represented by Eq. (7) [22].

$$V_{ij}^{t+1} = V_{ij}^t + d * r \quad (7)$$

where, g , d , and r corresponds to the inertia weight, the nuptial dance, and the damping ratio, respectively and represents a random value that falls within the range of -1 to 1.

ii) Movement of female mayflies

Unlike the male mayflies, the female mayflies do not form swarms themselves; instead, they fly towards the male mayfly swarms for the purpose of breeding. Let $P_{i,female}^t$ denote the current position of the i th female mayfly in a specific search dimension at time step t . The position altered by adding the velocity V_i^{t+1} to the current position. This can be represented using Eq. (8) [22].

$$P_{i,female}^{t+1} = P_{i,female}^t + V_i^{t+1} \quad (8)$$

where $P_{i,female}^0 \sim U(P_{min,female} - P_{max,female})$. The velocity, denoted as $V = (V_1, \dots, V_d)$, indicates how the position of mayfly changes over time. The direction in which the mayfly moves is determined through a dynamic interaction between the two individuals and their shared flying experiences. In this research, the method for attracting female mayflies involves locating the nearest male mayfly rather than employing random attraction. This approach aims to enhance the optimization convergence behaviour. As a result, the velocities of the female mayflies are determined using the equation provided in Eq. (9) [22].

$$V_{ij}^{t+1} = \begin{cases} V_{ij}^t + a_2 e^{-\beta r_{mf}^2} (P_{ij,male}^t - P_{ij,female}^t) & \text{if } f(P_{i,female}) > f(P_{i,male}) \\ V_{ij}^t + fl * r & \text{if } f(P_{i,female}) \leq f(P_{i,male}) \end{cases} \quad (9)$$

Similarly, the velocities of the male mayflies, V_{ij}^t signifies the velocity of the female mayfly in dimension j (where $j = 1, 2, \dots, n$) during the time step t . The variable $P_{ij,female}^t$ represents the position of the i -th female mayfly in dimension j at time t . The constant a_2 corresponds to positive attraction, while β is a fixed coefficient of visibility that determines the extent to which the mayfly's visibility is restricted to other mayflies. Additionally, the r_{mf} denotes the representation of Cartesian distance.

iii) Mating of mayflies

The algorithm incorporates a crossover operator for pairing male and female candidates. This involves the selection of two candidates from the population, which can be based on either their cost values or chosen randomly. Subsequently, the best couple breed with each other, and this cycle of breeding within the next generation continuous. The new generation, also known as offspring is derived using the Eq. (10) [22].

$$\begin{aligned} offspring_1 &= \gamma * male + (1 - \gamma) * female \\ offspring_2 &= \gamma * female + (1 - \gamma) * male \end{aligned} \quad (10)$$

Here, γ signifies a random value ranging from 0 to 1, while $\gamma * male$ and $\gamma * female$ represent the male and female parent candidates. The initial velocity of the offspring is initialized to zero.

3. Results and Discussions

In this study, the HFP models were developed using traditional and swarm intelligence algorithms, namely RLS and MA, respectively. These models were structured using an auto-regressive with exogenous (ARX) framework to depict the outcomes of the developed model in the form of transfer function. From the experiments conducted, 5000 input-output vibration datasets were selected, which were subsequently divided evenly into two segments. The initial 2500 data points were employed for model training, while the remaining 2500 data points were dedicated to test the developed model's performance.

Next, The HFP models that were developed underwent a validation process through mean squared error (MSE), pole-zero diagram analysis, and correlation testing. The selection of the most suitable model was primarily based on the outcomes of robustness assessments, prioritizing factors specifically in achieving the lowest MSE, demonstrating high stability, and obtaining unbiased results in the correlation tests. These assessments were conducted to ensure the exceptional performance

of the developed model. The optimal model was accomplished through a heuristic approach, given the absence of prior knowledge regarding the actual model order for the HFP system [23].

3.1 Modelling of HFP using RLS

In the process of modelling using the conventional RLS algorithm, two key parameters, namely the forgetting factor and model order, were thoroughly adjusted to achieved a robust model for the HFP system. The forgetting factor was fine-tuned within the range of 0.2 to 0.8, while the model order was systematically varied from 2 to 20. The outcome of this tuning procedure indicated that the most suitable model was achieved at the order 14, with a forgetting factor set at 0.8, resulting in the lowest MSE values of 3.7392×10^{-6} for the testing datasets. Figures 2(a) depicts both actual and estimated RLS outputs in the time domain, whereas Figure 2(b) offers a closer view at the results, specifically within the sample range of 2400 to 2600, providing enhanced visibility for observation. Additionally, Figure 3 presents the results in the frequency domain, displaying the natural frequencies of the first three modes of vibration in decibels (dB). According to the visual representations, the developed HFP model effectively replicates the characteristics of the actual system. This is evident in the overlapping of estimated output with the actual output. Moreover, the discrepancy between the actual and estimated RLS outputs is shown in Figure 4.

Correlation tests and assessment on its stability in pole-zero diagram were conducted to evaluate the efficiency of the model system achieved. Figure 5(a) indicates that the auto-correlation outcomes from the RLS modelling exceeded the 95% confidence level, suggesting bias result. However, the cross-correlation highlighted in Figure 5(b) revealed that the RLS modelling was unbiased, as the developed model fell within the 95% confidence level. The pole-zero diagram in Figure 6 reveals that the model exhibits stability, with all poles of the transfer function situated within the unit circle. Finally, the discrete transfer function resulting from the optimal RLS model is defined in Eq. (11).

$$\frac{y(t)}{u(t)} = \frac{0.01527z^{-1} + 0.06862z^{-2} + 0.08078z^{-3} + 0.01027z^{-4} - 0.09732z^{-5} - 0.148z^{-6} - 0.107z^{-7} - 0.01457z^{-8} + 0.06594z^{-9} + 0.08618z^{-10} + 0.04845z^{-11} + 0.002782z^{-12} + 0.002323z^{-13} + 0.04746z^{-14}}{1 - 0.09507z^{-1} + 0.008669z^{-2} + 0.0723z^{-3} + 0.07151z^{-4} + 0.03964z^{-5} + 0.01104z^{-6} + 0.01637z^{-7} + 0.05073z^{-8} + 0.07053z^{-9} + 0.02882z^{-10} - 0.07151z^{-11} - 0.1519z^{-12} - 0.1319z^{-13} - 0.03428z^{-14}} \quad (11)$$

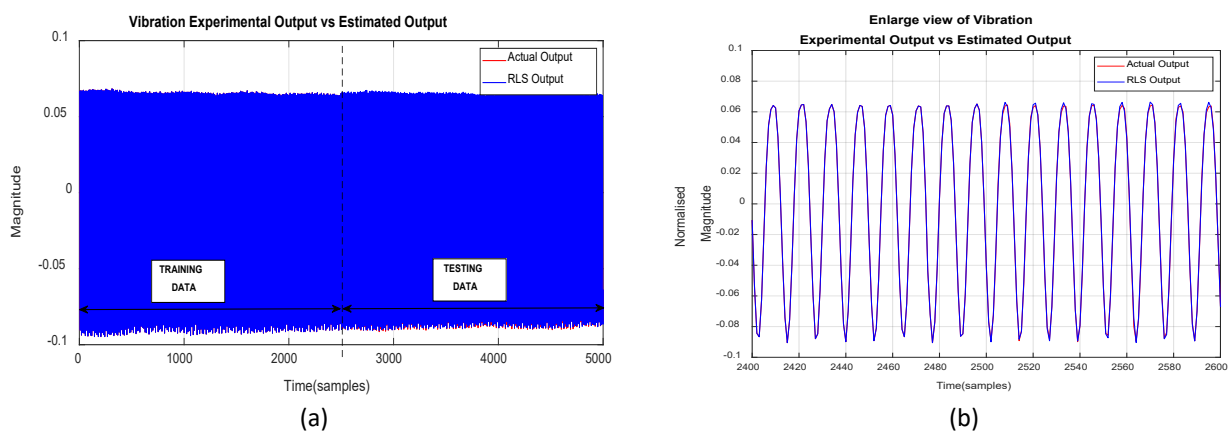


Fig. 2. Time domain for experimental and predicted output of the horizontal flexible plate via RLS: (a) 5000 selected data (b) Magnified view of the data from 2400 to 2600

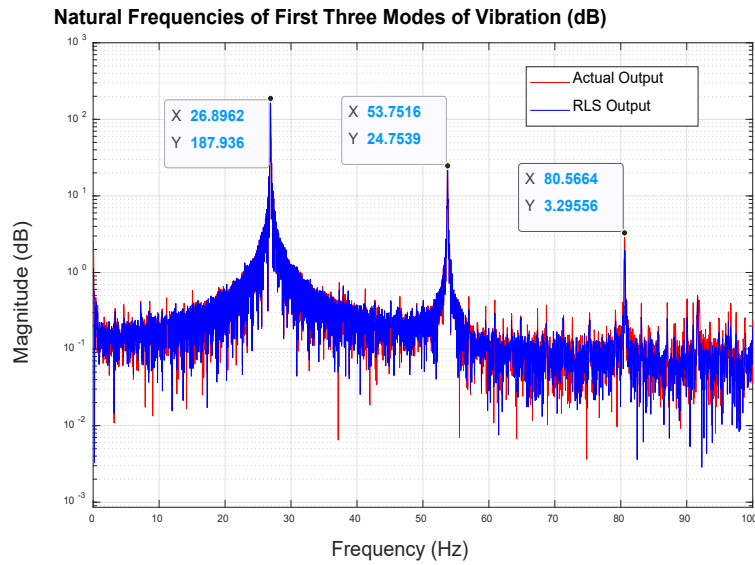


Fig. 3. The frequency domain for experimental and predicted outputs of the system using RLS

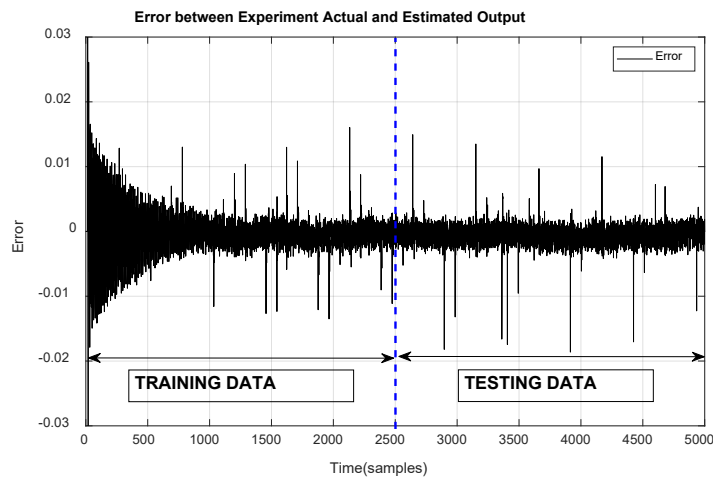


Fig. 4. The MSE between experimental and prediction outputs of the horizontal flexible plate via RLS modelling

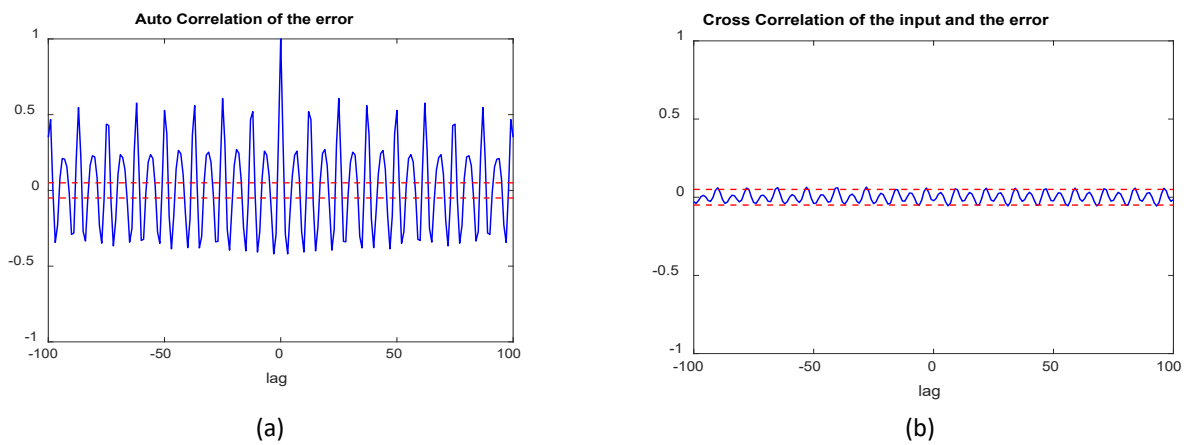


Fig. 5. The correlation test for RLS model in (a) auto-correlation (b) cross-correlation

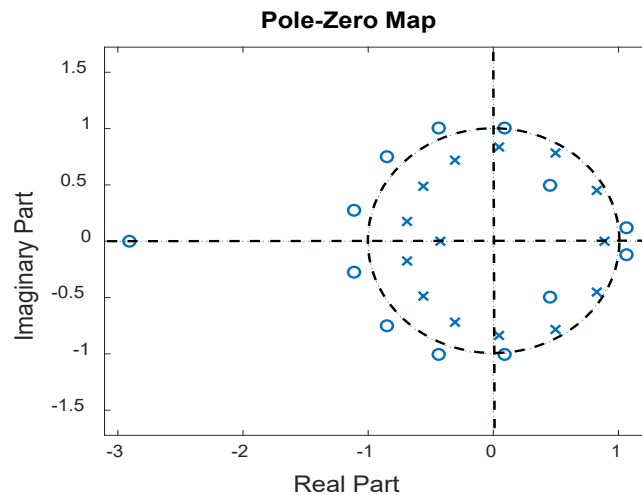


Fig. 6. The stability of RLS model using pole-zero map

3.2 Modelling of HFP using MA

The robust model of HFP utilizing swarm intelligence algorithm via MA was achieved by fine-tuning seven key parameters including population size, lower and upper bound, random flight, nuptial dance, inertia weight, model order, and maximum iteration. The parameters were systematically tuned using a heuristic approach. Initially, the size of population was adjusted within the range of 20 to 160, aligning with recommendations from Zervoudakis and Tsafar [22, 24] which have been found effective for various optimization problems. Once the optimal population size was determined, the remaining parameters were adjusted accordingly. Table 2 summarizes the range of parameter values that were fine-tuned, along with the optimal values identified during this study. These specific parameter settings were selected because they marked the convergence point where the MA algorithm had achieved its robust outcomes.

Table 2

The parameters setting for the best horizontal flexible plate model using MA

Parameters	Range of tuning values	Optimum Parameter
Population size, N_{pop}	20 - 160	40
[Lower boundary, Upper boundary]	[-1, 1] to [-10, 10]	[-9,9]
Random flight, fl	0.1 – 0.9	0.1
Nuptial dance, d	0.1 – 4.5	5
Inertia weight, g	0.9 – 9.99	5
Inertia weight damping ratio, g_{damp}	Fixed Variables	1
Attraction constant, a_1	Fixed Variables	1
Attraction constant, a_2	Fixed Variables	1.5
Attraction constant, a_3	Fixed Variables	1.5
Visibility coefficient, β	Fixed Variables	2
Random flight damping ratio, fl_{damp}	Fixed Variables	0.99
Mutation rate, mu	Fixed Variables	0.01
Dance damping ratio, $dance_damp$	Fixed Variables	0.8
Model order	3 – 10	4
Maximum generation, max_{iter}	100 – 500	400
Mean squared error for testing data	-	5.5186×10^{-6}

From all the tested model orders, the best model for the HFP plate system was determined to be of order 4. The MSE for the optimal MA algorithm model stands at 5.5186×10^{-6} attained from testing datasets. Figure 7 displays the convergence of the MA algorithm modelling during the simulation. Furthermore, Figures 8(a) and 8(b) illustrate both the actual and estimated MA outputs in time domain, covering overall datasets and a sample range of 2400 to 2600, respectively. Figure 9 presents outcomes in the frequency domain, demonstrating that the HFP model developed using MA algorithm effectively imitates the behaviors of the actual system, as indicated by the overlap between the estimated and actual outputs. Furthermore, Figure 10 reveals the error between the actual and predicted MA outputs.

The effectiveness of the developed model was verified through auto and cross-correlation tests, along with the pole-zero diagram assessment. Figures 11(a) and 11(b) reveal that both auto and cross-correlation results signified unbiased MA modeling, as the developed model remained within the 95% confidence level. In Figure 12, all poles of the transfer function located in the unit circle, indicating the stability of the developed model. Finally, Eq. (12) provides the derived discrete transfer function obtained from the optimal MA model.

$$\frac{y(t)}{u(t)} = \frac{-0.3929z^{-1} + 0.3088z^{-2} + 0.4256z^{-3} - 0.8195z^{-4}}{1 - 1.118z^{-1} + 0.4077z^{-2} - 0.1119z^{-3} + 0.09016z^{-4}} \quad (12)$$

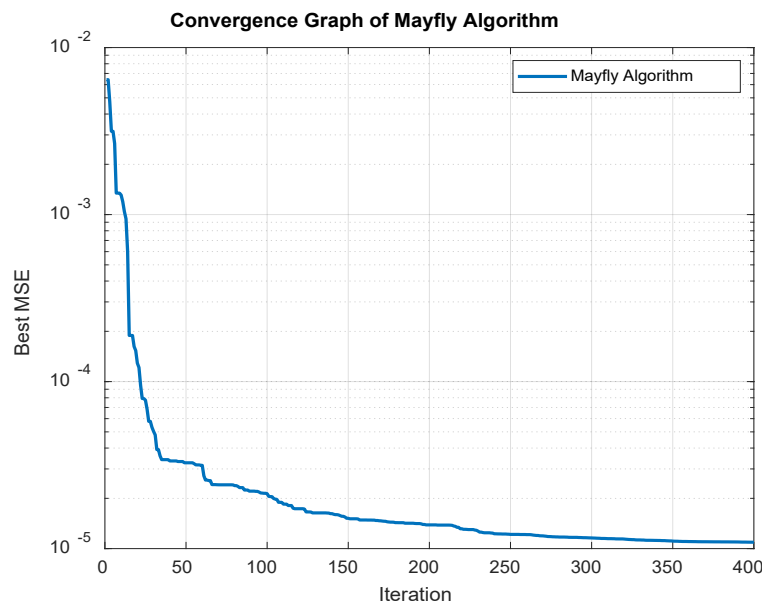


Fig. 7. The convergence graph of predicted model via MA

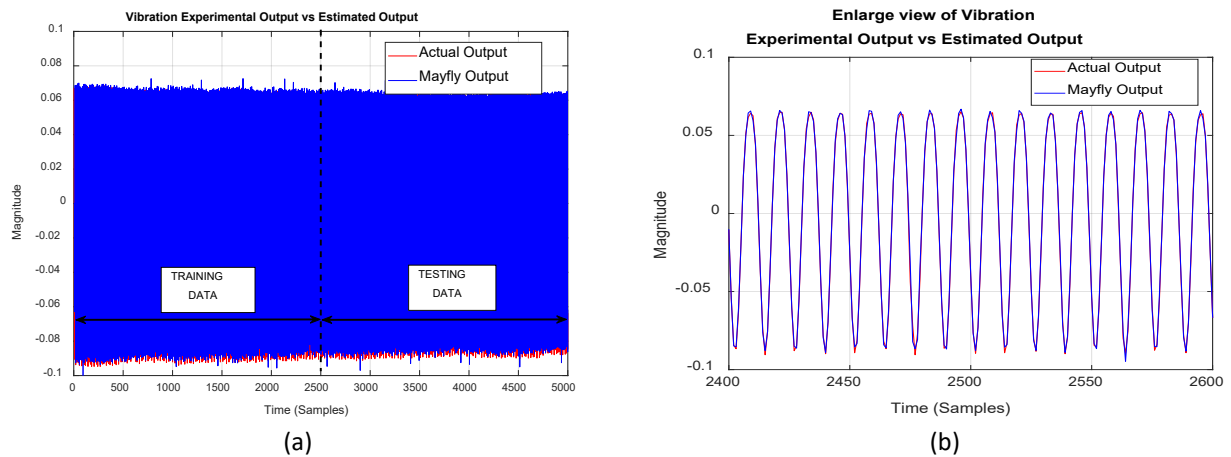


Fig. 8. Time domain for experimental and predicted output of the horizontal flexible plate via MA:
(a) 5000 selected data (b) Enlarge view of the data from 2400 to 2600

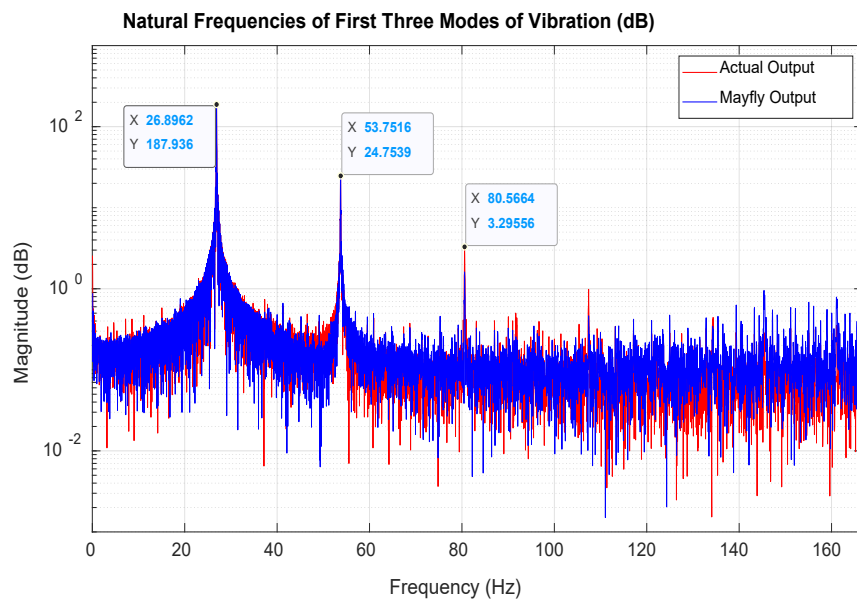


Fig. 9. The frequency domain for experimental and predicted outputs of the system using MA

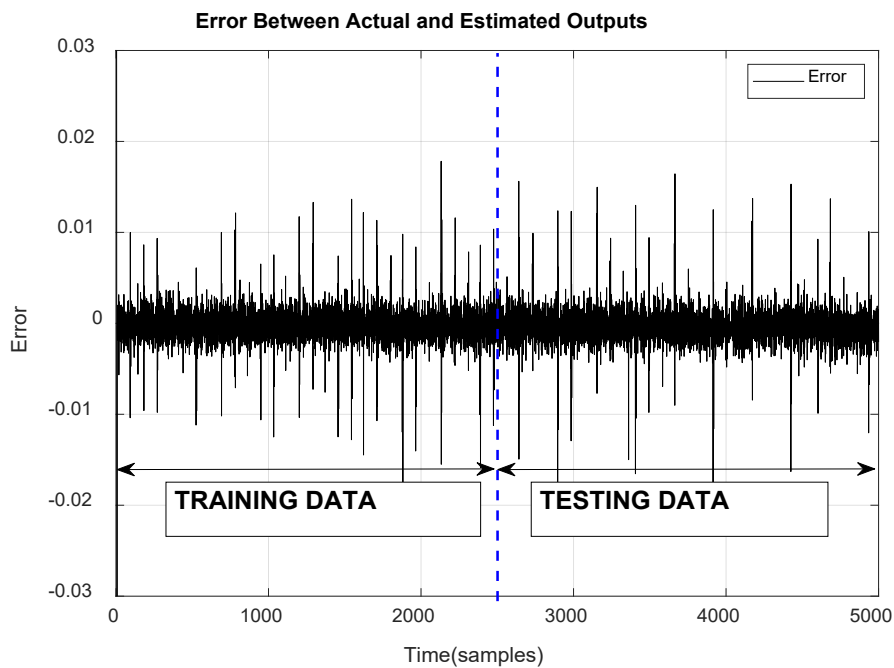


Fig. 10. The MSE between experimental and prediction outputs of the horizontal flexible plate via MA modelling

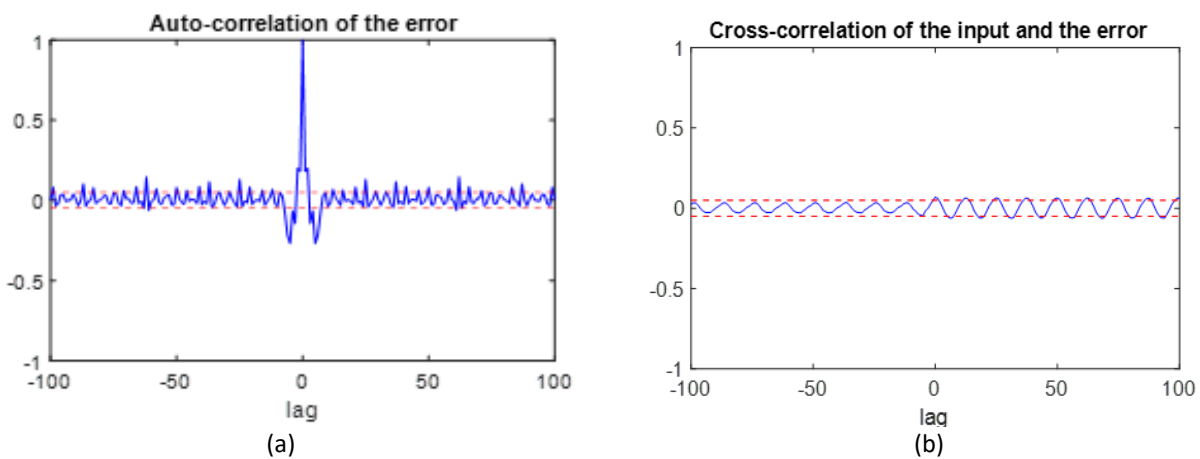


Fig. 11. The correlation test for MA model in (a) auto-correlation (b) cross-correlation

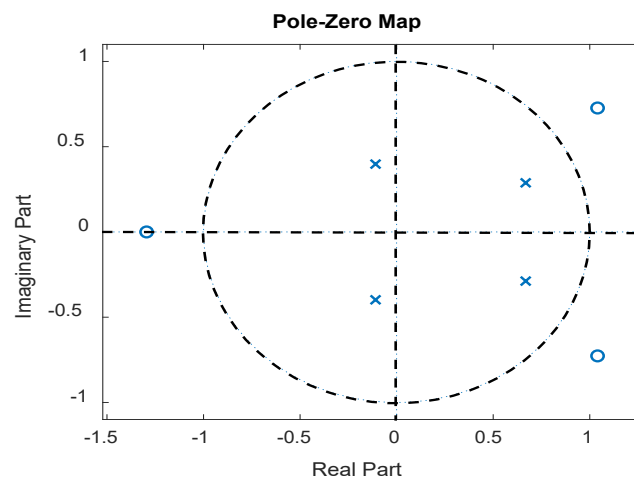


Fig. 12. The stability of MA model using pole-zero map

3.3 Comparative Assessment between RLS and MA Modelling

The performance of all the developed models was assessed to identify the most suitable model for representing the flexible plate system. According to the results, the lowest MSE values for RLS and MA algorithms were 3.7392×10^{-6} and 5.5185×10^{-6} , respectively. Notably, the MSE values for both algorithms were relatively close to each other, however, two additional validations are required before selecting the optimal model.

The results of correlation tests indicate that the MA algorithm exhibited unbiased behaviour in both auto and cross correlation tests, correlating within a 95% confidence level. On the other hand, the RLS algorithm was only found to be unbiased in the cross-correlation test. Following the stability analysis using the pole-zero diagram, it was observed that all models were stable, as evidenced by all poles residing within the unit circle.

Through various validation methods, the performance of SIA via MA outperformed the traditional algorithm using RLS in modelling the flexible plate system. Additionally, SIA yielded transfer functions with lower orders compared to conventional algorithms. Previous research has emphasized the importance of constructing simple models that retain essential system attributes [25].

In this study, SIA generated models with orders of 4, while RLS produced models with orders of 14. Therefore, SIA represents the simplest model which capable of providing a simple transfer function for better control strategies. This indicates that SIA offer more effective insights into the behaviour of the flexible plate system compared to traditional approaches. The remarkable performance of the MA algorithm can be attributed to its sophisticated optimization strategy, which uniquely combines elements from various algorithms.

The algorithm ability to swiftly converge to optimal solutions surpasses traditional approaches, providing a clear advantage in modelling flexible plate model. In delineating the framework and methodology of the MA algorithm, it becomes evident that its approach significantly differs from conventional methods. The incorporation of innovative components and adaptive strategies enables MA to capture the intricacies of the flexible plate systems more effectively, thus outperforming the traditional RLS algorithm.

In light of the findings and insights gained from this study, it is imperative to acknowledge its limitations. Firstly, the focus was primarily on this specific algorithm, which may not be universally suitable for all flexible structures. Future research should explore its adaptability to different scenarios and conditions. Secondly, the experimental setup, while suitable for our objectives, is limited in its representation of real-world conditions. Further investigation should encompass a broader range of boundary conditions and excitation methods. Additionally, the parameterization of MA is critical, and the impact of parameter choices on performance requires further exploration.

Future research endeavours should encompass a broader spectrum of structural scenarios to assess the adaptability and robustness of the Mayfly Algorithm (MA) in modelling various flexible structures. Additionally, an in-depth investigation into parameter optimization techniques is essential to enhance MA's modelling efficiency and accuracy across different applications. Beyond modelling, exploring the integration of MA-based models into real-time control systems for adaptive structural control represents a promising avenue. This research direction holds the potential to not only expand the practical applicability of MA in structural engineering but also contribute to more efficient and adaptive control strategies for flexible structures.

4. Conclusions

This research provides a thorough investigation into the dynamic behaviours of a HFP structure. It explores two distinct modelling approaches, which were traditional and metaheuristic. In this study, two algorithms were employed, specifically RLS and MA to represent the traditional and metaheuristic strategies, respectively. An extensive evaluation of both models and their respective performances were discussed in-depth. The models derived through the employment of MA and RLS algorithms were acquired, verified, found to be acceptable, and can be considered suitable for future utilization in developing controllers aimed at suppressing undesired vibrations acting upon a HFP system. It is worth noting that the RLS modelling results achieved the lowest MSE compared to MA in this research. However, MA adeptly captured the system characteristics by demonstrating strong correlations in the test results, and displaying high stability in the pole-zero diagram when compared to the RLS. These validations are of utmost importance in gauging the effectiveness of the developed models. In conclusion, it can be inferred that the MA has effectively approximated the model of the HFP with clamped boundary conditions on all edges. Future research could explore the integration of multiple optimization algorithms to enhance the accuracy and efficiency of modelling the dynamic behaviour of flexible plate structures. Combining the strengths of both traditional and metaheuristic approaches, along with the potential inclusion of machine learning techniques, it could lead to more robust and adaptable modelling solutions. This hybrid approach could provide better results, especially in complex scenarios or when dealing with noisy data.

Acknowledgement

The authors would like to express their gratitude to the Minister of Higher Education Malaysia (MOHE), Universiti Malaysia Sarawak (UNIMAS), and Universiti Teknologi MARA for funding and providing facilities to conduct this study.

References

- [1] Erb, Randall M., Jonathan S. Sander, Roman Grisch, and André R. Studart. "Self-shaping composites with programmable bioinspired microstructures." *Nature communications* 4, no. 1 (2013): 1712. <https://doi.org/10.1038/ncomms2666>
- [2] Zhang, Yuxiang, and Hortense Le Ferrand. "Bioinspired self-shaping clay composites for sustainable development." *Biomimetics* 7, no. 1 (2022): 13. <https://doi.org/10.3390/biomimetics7010013>
- [3] Leira, B. J. and Moan, T. "Hydroelastic analysis of a flexible plate in viscous flow." *Journal of Fluids and Structures*, 56 (2015): 60-81.
- [4] Mondal, M., Kamsma, P. and Diaz, V. H. "Investigation of flexible plate structures for wind energy conversion." *Energy Procedia* 75 (2015): 2486-2493.
- [5] Abd Al Rahman, M., and Alireza Mousavi. "A review and analysis of automatic optical inspection and quality monitoring methods in electronics industry." *Ieee Access* 8 (2020): 183192-183271. <https://doi.org/10.1109/ACCESS.2020.3029127>
- [6] Hadi, Muhamad Sukri, Hanim Mohd Yatim, and Intan Zaurah Mat Darus. "Modelling and control of horizontal flexible plate using particle swarm optimization." *International Journal of Engineering & Technology* 7, no. 2.29 (2018): 13. <https://doi.org/10.14419/ijet.v7i2.29.13117>
- [7] Nazri, S. S. Z., M. S. Hadi, H. M. Yatim, M. H. Ab Talib, and I. Z. M. Darus. "Modelling of Flexible Manipulator System via Ant Colony Optimization for Endpoint Acceleration." In *Journal of Physics: Conference Series*, vol. 2129, no. 1, p. 012016. IOP Publishing, 2021. <https://doi.org/10.1088/1742-6596/2129/1/012016>
- [8] Ali, Siti Khadijah, Mohamad Faisal Fadzilan, Aida Nur Syafiqah Shaari, Muhamad Sukri Hadi, Rickey Ting Pek Eek, and Intan Zaurah Mat Darus. "Modelling of flexible beam based on ant colony optimization and cuckoo search algorithms." *Journal of Vibroengineering* 23, no. 4 (2021): 810-822. <https://doi.org/10.21595/jve.2020.21730>
- [9] Mohammed, Mohammed Jawad, Majida Khalil Ahmed, and Basma Abdullah Abbas. "Modeling and control of horizontal flexible plate using PID-CS controller." *Journal of Mechanical Engineering Research and Developments (JMERE)* 24, no. 4 (2019): 138-142. <https://doi.org/10.26480/jmerd.04.2019.138.142>

- [10] Sariyildiz, Emre, Haoyong Yu, and Kouhei Ohnishi. "A practical tuning method for the robust PID controller with velocity feed-back." *Machines* 3, no. 3 (2015): 208-222. <https://doi.org/10.3390/machines3030208>
- [11] Shaari, Aida Nur Syafiqah, Muhamad Sukri Hadi, Abdul Malek Abdul Wahab, Rickey Ting Pek Eek, and Intan Zaurah Mat Darus. "Active vibration control of flexible beam system based on cuckoo search algorithm." *International Journal of Electrical & Computer Engineering (2088-8708)* 13, no. 2 (2023). <https://doi.org/10.11591/ijece.v13i2.pp2289-2298>
- [12] Gao, Zheng-Ming, Su-Ruo Li, Juan Zhao, and Yu-Rong Hu. "The guaranteed convergence mayfly optimization algorithm." In *2020 7th International Forum on Electrical Engineering and Automation (IFEEA)*, pp. 858-861. IEEE, 2020. <https://doi.org/10.1109/IFEEA51475.2020.00179>
- [13] Maseri, Siti Zakiah, Muhamad Sukri Hadi, Annisa Jamali, Hanim Mohd Yatim, Mat Hussin Ab Talib, and Intan Zaurah Mat Darus. "A Single objective flower pollination algorithm for modeling the horizontal flexible plate system." In *2019 2nd International Conference on Applied Engineering (ICAE)*, pp. 1-6. IEEE, 2019. <https://doi.org/10.1109/ICAE47758.2019.9221652>
- [14] Hassan, M. H., A. Jamali, M. S. Z. M. Suffian, M. S. Hadi, and IZ Mat Darus. "Grey Wolf Optimization For Intelligent Parametric Modeling Of Gradient Flexible Plate Structure." *Journal of Applied Science and Engineering* 26, no. 9 (2022): 1207-1214. [https://doi.org/10.6180/jase.202309_26\(9\).0001](https://doi.org/10.6180/jase.202309_26(9).0001)
- [15] Ahmed, Aram M., Tarik A. Rashid, and Saeed Soran Ab M. "Cat swarm optimization algorithm: a survey and performance evaluation." *Computational intelligence and neuroscience* 2020 (2020). <https://doi.org/10.36227/techrxiv.11656458.v1>
- [16] Liu, Yuhu, Yi Chai, Bowen Liu, and Yiming Wang. "Bearing fault diagnosis based on energy spectrum statistics and modified mayfly optimization algorithm." *Sensors* 21, no. 6 (2021): 2245. <https://doi.org/10.3390/s21062245>
- [17] Elavarasan, G., K. S. Kumar, M. Marimuthu, K. Narayanasamy, and R. P. Selvam. "Evolutionary oppositional mayfly optimization based task scheduling algorithm for cloud computing." *Turk. J. Physiother. Rehabil* 32 (2021): 3800-3806.
- [18] Oladimeji, A. I., A. W. Asaju-Gbolagade, and K. A. Gbolagade. "A proposed framework for face-iris recognition system using enhanced mayfly algorithm." *Nigerian Journal of Technology* 41, no. 3 (2022): 535-541. <https://doi.org/10.4314/njt.v41i3.13>
- [19] Zhang, Tian, Yongquan Zhou, Guo Zhou, Wu Deng, and Qifang Luo. "Bioinspired bare bones mayfly algorithm for large-scale spherical minimum spanning tree." *Frontiers in Bioengineering and Biotechnology* 10 (2022): 830037. <https://doi.org/10.3389/fbioe.2022.830037>
- [20] Du, Qianhang, and Honghao Zhu. "Dynamic elite strategy mayfly algorithm." *PloS one* 17, no. 8 (2022): e0273155. <https://doi.org/10.1371/journal.pone.0273155>
- [21] Kadry, Seifedine, Venkatesan Rajinikanth, Jamin Koo, and Byeong-Gwon Kang. "Image multi-level-thresholding with Mayfly optimization." *International Journal of Electrical & Computer Engineering (2088-8708)* 11, no. 6 (2021). <https://doi.org/10.11591/ijece.v11i6.pp5420-5429>
- [22] Zervoudakis, Konstantinos, and Stelios Tsafarakis. "A mayfly optimization algorithm." *Computers & Industrial Engineering* 145 (2020): 106559. <https://doi.org/10.1016/j.cie.2020.106559>
- [23] Hadi, M. S., and IZ Mat Darus. "Intelligence swarm model optimization of flexible plate structure system." *International review of automatic control* 6, no. 3 (2013): 322-331.
- [24] Patil, Ratna, Sharvari Tamane, Shitalkumar Adhar Rawandale, and Kanishk Patil. "A modified mayfly-SVM approach for early detection of type 2 diabetes mellitus." *Int. J. Electr. Comput. Eng* 12, no. 1 (2022): 524-33. <https://doi.org/10.11591/ijece.v12i1.pp524-533>
- [25] Billings, Stephen A. *Nonlinear system identification: NARMAX methods in the time, frequency, and spatio-temporal domains*. John Wiley & Sons, 2013. <https://doi.org/10.1002/9781118535561>